



HAL
open science

MRI assessment of treatment delivery for interstitial photodynamic therapy of high-grade glioma in a preclinical model

Henri-Arthur Leroy, Maximilien Vermandel, Bertrand Leroux, Alain Duhamel, Jean-Paul Lejeune, Serge Mordon, Nicolas Reyns

► To cite this version:

Henri-Arthur Leroy, Maximilien Vermandel, Bertrand Leroux, Alain Duhamel, Jean-Paul Lejeune, et al.. MRI assessment of treatment delivery for interstitial photodynamic therapy of high-grade glioma in a preclinical model. *Lasers in Surgery and Medicine*, 2017, Epub ahead of print. 10.1002/lsm.22744 . inserm-01616405

HAL Id: inserm-01616405

<https://inserm.hal.science/inserm-01616405>

Submitted on 13 Oct 2017

HAL is a multi-disciplinary open access archive for the deposit and dissemination of scientific research documents, whether they are published or not. The documents may come from teaching and research institutions in France or abroad, or from public or private research centers.

L'archive ouverte pluridisciplinaire **HAL**, est destinée au dépôt et à la diffusion de documents scientifiques de niveau recherche, publiés ou non, émanant des établissements d'enseignement et de recherche français ou étrangers, des laboratoires publics ou privés.

MRI assessment of treatment delivery for interstitial photodynamic therapy of high-grade glioma in a preclinical model

Authors:

Henri-Arthur Leroy, MD^{1, 2*}, Maximilien Vermandel, PhD^{1*}, Bertrand Leroux¹, Alain Duhamel, PhD³, Jean-Paul Lejeune, MD, ^{1, 2}, Serge Mordon PhD¹, Nicolas Reyns, MD, PhD^{1, 2}

Affiliations:

¹ Univ. Lille, INSERM, CHU Lille, U1189 - ONCO-THAI - Image Assisted Laser Therapy for Oncology, F-59000 Lille, France

² Department of Neurosurgery, University Hospital, Lille, France

⁵ Department of Biostatistics, EA2694, UDSL, University of Lille, University Hospital, Lille, France

* These authors contributed equally to the publication and are co-first authors.

Corresponding author:

Dr. Maximilien Vermandel

INSERM U1189 - ONCO-THAI

University of Lille - CHRU de Lille

1, Avenue Oscar Lambret

Email: m-vermandel@chru-lille.fr

Phone number: 0033 3 20 44 67 21

Compliance with ethical standards:

Conflicts of interest: None.

Funding: Financial support by the University of Lille and INSERM.

Ethical approval: This article contains studies using animals. All applicable institutional and national guidelines for the care and use of animals were followed. The experimental design was declared to the French National Ethics Committee under reference number 04870.01.

Acknowledgments: The authors warmly thank Florent Auger and Nicolas Durieux for their helpful support in acquiring the MR images.

Abstract

Background

High-grade gliomas are primary brain tumors that have shown increasing incidence and unfavorable outcomes. Local control is crucial to the management of this pathology. Photodynamic therapy (PDT), based on the light-induced activation of a photosensitizer (PS), achieves local treatment by inducing selective lesions in tumor tissue.

Objectives

Previous studies have reported the outcomes of PDT for glioblastoma via immunohistological data. Our study aimed to evaluate MRI findings, including diffusion and perfusion sequences, compared with immunohistological data from the same population to address the efficiency of light fractionation.

Materials and Methods

Twenty-six “nude” rats grafted with human U87 cells into the right putamen underwent PDT. After PS precursor (5-ALA) intake, an optical fiber was introduced into the tumor. The rats were randomized into the following groups: those without illumination and those that received two or five fractions of light. Treatment effects were assessed with early high-field MRI to measure the volume of necrosis and edema using diffusion and perfusion sequences; the MRI results were compared with immunohistology results, including necrosis and apoptosis markers.

Results

Elevated diffusion values were observed on MRI in the centers of the tumors of the treated animals, especially in the 5-fraction group ($p < 0.01$). Perfusion was decreased around the treatment site, especially in the 5-fraction group ($p = 0.024$). The MRI findings were consistent with previously published histological data. The median volume of necrosis was significantly different between the sham group and treated groups, 0 mm^3 vs. 2.67 mm^3 , $p < 0.001$. The same trend was previously observed in histology data when grading the absence or presence of necrosis and when the presence of necrosis was significantly more predominant for the treated group than for the untreated group ($p < 0.001$). Additionally, cell death represented by apoptosis marker data (TUNEL method) was significantly higher in the 5-fraction group than in the 2-fraction group ($p = 0.01$).

Conclusion

Diffusion and perfusion MRI revealed histological lesions. Interstitial PDT induced specific lesions in the tumor tissue, which were observed with MRI and confirmed by histopathological analysis. Thus, MRI may provide a non-invasive and reliable tool to assess treatment outcomes after PDT.

Keywords: 5-ALA, PpIX, Photodynamic Therapy, Magnetic Resonance Imaging, PDT, MRI, Glioblastoma, High-Grade Glioma

I. Introduction

Primary brain tumors are the second most common cause of cancer death in young men (20 to 39 years old) and the fourth most common cause of cancer in young women⁹. Currently, the incidence of high-grade glioma is greater than 5 per 100,000 people, and this disease leads to 3% of all cancer deaths for patients aged 35 to 64 years¹¹. Among these tumors, glioblastoma (GBM) remains the primitive cerebral tumor (WHO grade IV) with the worst prognosis. GBM management relies on maximal resection followed by concomitant radio-chemotherapy. Nevertheless, patients harboring GBM still have poor prognoses and median survival (15 months)^{8,12}. Local control is crucial for improving progression-free and overall survival. Photodynamic therapy (PDT) using 5-aminolevulinic acid (5-ALA) might address some issues of local control. Indeed, recent studies have reported a significant increase in overall survival, of up to 4 years, in patients treated with interstitial PDT (iPDT)^{1,14}. iPDT, which consists of guiding optical fibers under stereotactic conditions to the tumor site, is particularly relevant, especially for non-resectable GBM.

After several enzymatic transformations (i.e., heme biosynthesis), 5-ALA is transformed into protoporphyrin IX (PpIX), which is the photoactive compound involved in PDT. PpIX has a broad absorption spectrum. The maximal absorption peak is in the blue region; however, 635 nm is generally considered the optimal excitation wavelength for PDT as it penetrates deeper into the tissue than other wavelengths. After PpIX is excited, the following types of reactions occur: 1) free radical production and 2) oxidative species formation⁶. Here, the presence of oxygen is required to achieve photodynamic interactions. Thus, treatment delivery should involve tissue oxygenation to increase the therapeutic effects³. Fractionation (i.e., alternating the on / off period of light) might address this issue⁴. Accordingly, Tétard et al. previously reported data suggesting an improvement in the PDT effect after fractionated PDT compared with continuous illumination¹⁶.

The main objective of our study was to evaluate how MRI contributes to the assessment of fractionated PDT delivery.

In a previous study¹⁰, we demonstrated that light fractionation during iPDT enhances therapeutic effects. Our previous study assessed the effects of interstitial-fractionated 5-ALA PDT, using histopathological analysis, in a preclinical GBM model. In the present study, we focused on non-invasive techniques to assess the treatment outcomes. Multiparametric MRI was combined with immunohistological analyses from a previous study using the same population. High-field MRI acquisition was performed at the same time as previous experiments. In this context, diffusion and perfusion, in addition to conventional sequences including gadolinium enhancement, were investigated to assess the reliability of multiparametric MRI in iPDT, compared to histological analyses.

II. Materials and methods

The comparison was made using a histology study conducted after a specific treatment scheme in which different effects were clearly observed between two treatment protocols using two or five light fractions. Furthermore, these two groups were compared to a baseline group identified as a sham group with no illumination.

The entire protocol, including ethical considerations, the grafting procedure, and treatment delivery, was presented in a previous study ¹⁰.

Twenty-six nude rats (phenotype Fox n1 rnu/rnu, from Charles River[®], partially immuno-compromised) underwent surgical grafting. Cells with DMEM alone (5 μ l containing 5×10^5 human GBM U87 cells) were grafted using stereotactic conditions, which allow high precision and reproducibility. PDT was delivered under MRI guidance after 5-ALA intake. To deliver illumination, a silica optical fiber, UltraSil 272 ULS (OFS, Norcross, GA, USA), which had an outside diameter of 350 μ m and a numerical aperture of 0.29, was inserted into the brain through the cannula of the anchor at the predetermined depth (upper third of the tumor). No illumination was administered to specimens in the sham group. For the other groups, 25 J of illumination was delivered at 30 mW/cm² at a wavelength of 635 nm. The 2-fraction group specimens were exposed to 5 J first, and the remaining 20 J was administered after a pause of 2 min 30 s. The 5-fraction group specimens were exposed to 5 fractions of 5 J each, every 2 min 30 s.

a) Imaging protocol

For this study, images were acquired on a 7 Tesla MRI device (Bruker[®], Biospec, Ettlingen, Germany). Two types of antennae were used, depending on the configuration (i.e., image-guided therapy or diagnosis). Image-guided PDT was administered with a cylindrical transceiver antenna with a 72-mm internal diameter, while the diagnosis images were acquired with a surface antenna placed over the scalp of the animal for signal reception. During the imaging procedure, sedation was maintained using continuous isoflurane inhalation of approximately 2%, depending on the cardiac and respiratory frequencies.

MRI analyses were performed 7 days after U87 grafting to assess the engraftment. Then, MRI was repeated during the treatment and at 48-72 hours after PDT. A T2-weighted TurboRARE sequence ¹³ was systematically acquired in the axial plane to evaluate the geometry and position of the tumor. A T1-weighted sequence was performed routinely before and after gadolinium injection on the axial plane using the RARE type of spin echo. A perfusion sequence without contrast injection was performed before and after treatment. The arterial spin labeling (ASL) ¹⁹ method provided quantitative information on the tissue perfusion by magnetic labeling of blood entering the slice. This corresponded to the wash-in measurement. Tissue perfusion was measured on a single axial section of 850 μ m thickness, located at the tumor, in units of ml / (100 g tissue / min). Diffusion-weighted imaging (DWI) was also performed before and after treatment. This sequence provides information on the degrees of

freedom of the water molecules in the tissue. In our study, image acquisition for diffusion was achieved in 3D using the Echo-planar Imaging (EPI) technique, and the coefficient was measured on a single, 850- μm thick axial slice located at the tumor and was expressed in $\mu\text{m}^2/\text{sec}$.

The post-processing of MRI data for diffusion and perfusion sequences was performed using Paravision 5.1 software provided by the manufacturer (Bruker[®], Biospec, Ettlingen, Germany). Semi-quantitative measurements were performed. Thus, diffusion and perfusion values were computed from regions of interest (ROI) placed on the tumor and contralateral to the tumor (Striatum). The ratio between these two ROIs (tumor / healthy brain) was calculated before and after treatment, such that the delta (i.e., Δd for diffusion and Δp for perfusion) could be calculated (Eq. 1).

$$\Delta x = \frac{ratio_{post} - ratio_{pre}}{ratio_{pre}} \times 100\% \quad \text{Eq. 1}$$

x is the coefficient being observed according to the MRI sequence (i.e., diffusion or perfusion)

$$ratio_{pre} = \frac{x_{tumor_{pre}}}{x_{striatum_{pre}}} \text{ and } ratio_{post} = \frac{x_{tumor_{post}}}{x_{striatum_{post}}}$$

and $x_{tumor_{pre}}$, $x_{striatum_{pre}}$, $x_{tumor_{post}}$ and $x_{striatum_{post}}$ indicate the average coefficient x (i.e., diffusion or perfusion) measured for Tumor_ROI_pre, Striatum_ROI_pre, Tumor_ROI_post, and Striatum_ROI_post, respectively.

Morphological MRI analyses were conducted with OsiriX imaging software (64-bit version 3.8.1, Pixmeo[®], Geneva, Switzerland), which enabled the evaluation of the volumes of the treated tumors, as well as necrosis and peritumoral edema. The tumor volume was determined using the T1-weighted images after contrast injection. The tumor was manually delineated on each T1 gadolinium slice, and the volume was estimated according to the surface of each ROI taking into account the thickness of each slice. The volume of the peritumoral edema was segmented on T2 images. The change in the intratumoral signal on either the T2 or T1 gadolinium sequences was manually delineated to quantify necrosis.

b) Immunohistological analysis

As previously reported by Leroy et al.¹⁰, 19 tissue samples were subjected to immunohistological analysis. The histological slices of interest were selected in the optical fiber plane. MR images were analyzed and compared with the histology results, including necrosis, apoptosis staging with the TUNEL method (ApopTag[®] Plus Peroxidase In Situ, Millipore, USA) and edema.

c) Statistical analysis

The number of subjects required was estimated to obtain a statistical power of 80% with $\alpha = 5\%$. However, given the preliminary nature of this study and the absence of literature on this topic, other

preclinical studies were used to estimate the sample size, taking into account a 10-15% loss². More than 10 animals per group were estimated to be necessary.

Data are presented as the medians and interquartile ranges (IQR) (e.g., median volume measurements). Non-parametric tests were conducted due to the small sample sizes. The Wilcoxon Rank Sum test was performed to test the distribution symmetry among the samples. The Kruskal-Wallis test was used for comparisons among more than two independent groups. The Jonckheere-Terpstra trend test was conducted (e.g., diffusion gradient or perfusion, according to the allocated treatment) to compare independent groups with ordered alternatives. Fisher's exact test was used to compare the histological findings due to the small numbers of specimens (theoretical groups < 5). The data were analyzed with SAS software, version 9.3 (SAS Institute, Cary, NC).

Results

The 26 specimens harbored tumors that were sufficiently large for treatment. The median tumor volume, measured from T1 MRI, was 3.7 mm³ (range, 1.42 to 13). The median tumor volume did not differ significantly among the 3 groups ($p = 0.44$). Two out of 26 rats died within the 72-hour interval after PDT due to cerebral herniation or hydrocephalus; thus, the post-op histopathology and MRI analysis were unachievable for them. Concerning MRI examination, 24 specimens underwent post-PDT MRI (8 examinations per group). Concerning histology, 5 slides could not be interpreted because of aliasing artifacts or incorrectly fixed tissue. Thus, 19 tumor slides with H&E staining from the 26 treated rats were studied (5 for the 5-fraction group, 7 for the 2-fraction group and 7 for the sham group).

a) Diffusion

Among the 26 rats, 24 benefited from pre- and post-treatment diffusion sequences. Two rats died within 72 hours after iPDT, due to intracranial hypertension (due to high tumor volumes). All Δd values are represented in Figure 1. Median increases of 2.6% (IQR, 0.53, 5.39) in the sham group; 7.15% (IQR, -1.37, 18.1) in the 2-fraction group; and 19% (IQR 9.6, 33.4) in the 5-fraction group ($p < 0.01$) were obtained.

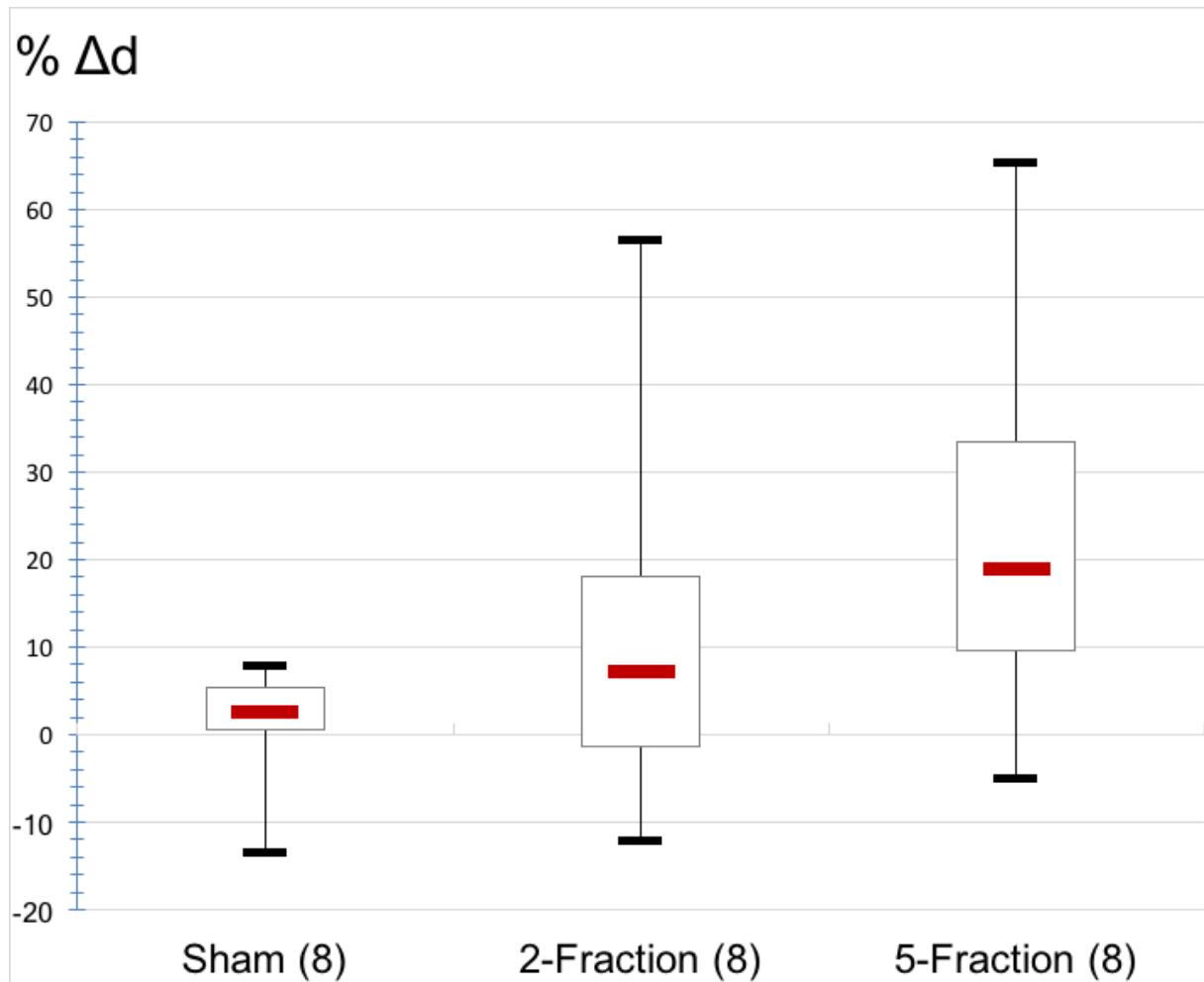


Figure 1: Boxplot illustrating variations in Δd for the sham, 2-fraction and 5-fraction groups (red marks represent the median, the size of the box is the IQR, and the minimum/maximum are indicated by black marks), the number of specimens per group is in brackets. The Jonckheere-Terpstra test result was significant, with a greater increase in Δd after PDT in the 5-fraction group ($p < 0.01$).

b) Perfusion

Among the 26 treated rats, 22 benefited from pre- and post-treatment perfusion sequences. All Δp values are represented in Figure 2. After calculating the Δp , median decreases of -23% (IQR -30.27; -15.31) in the sham group, -36% (IQR, -70.15; -3.23) in the 2-fraction group, and -61% (IQR, -69.1; -49.5) in the 5-fraction group ($p = 0.024$) were observed.

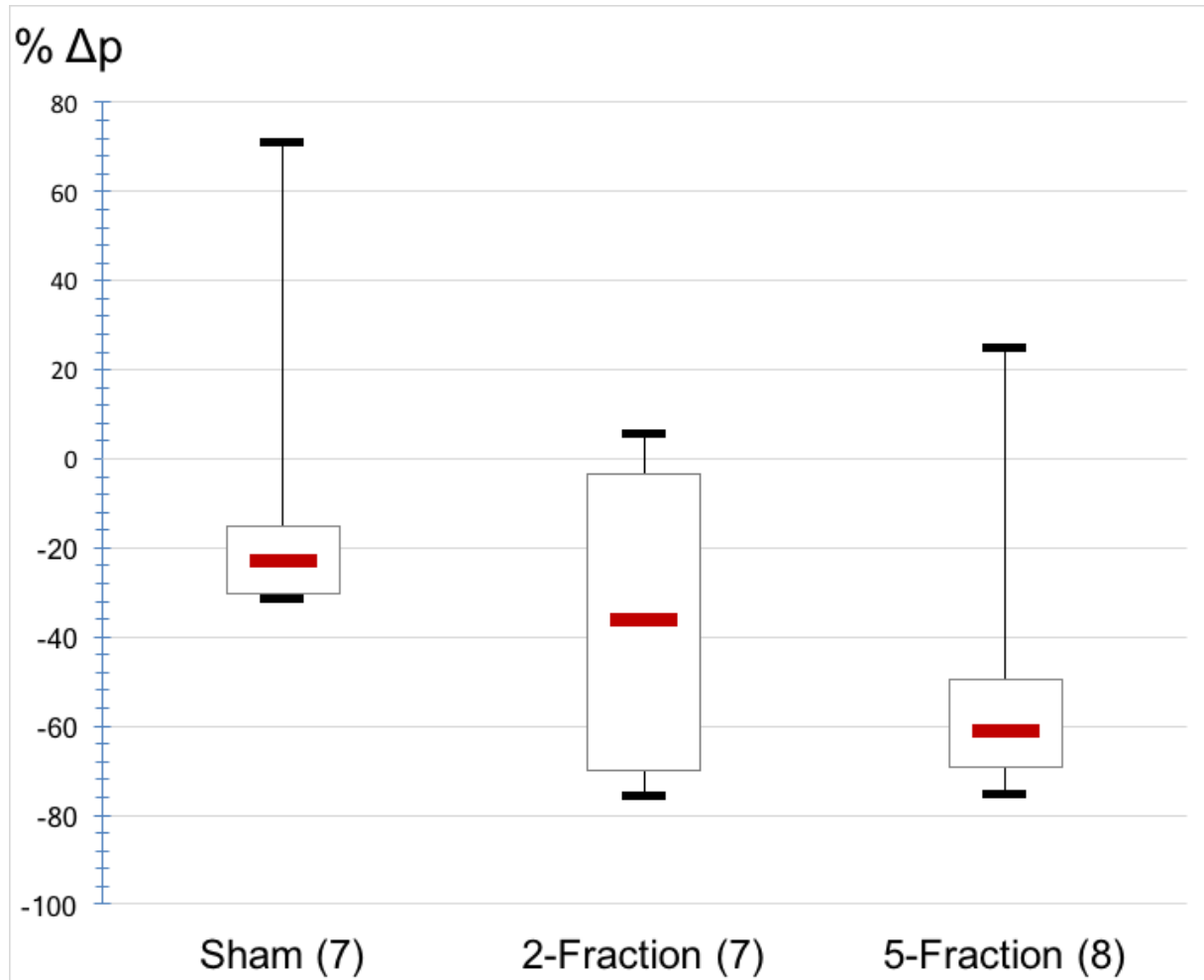


Figure 2: Boxplot illustrating variations in Δp for the sham, 2-fraction and 5-fraction groups (red marks represent the median, the size of the box is the IQR, and the minimum/maximum are indicated by black marks), the number of specimens per group is in brackets. The decrease in Δp after PDT was greater in the 5-fraction group ($p = 0.024$).

c) Necrosis volume

The median volume of necrosis was significantly different between the sham group and the treated groups, 0 mm^3 vs. 2.67 mm^3 , $p < 0.001$. However, no difference was found between the 2-fraction and 5-fraction groups, 2.53 mm^3 (IQR, 0.67; 5.57) vs. 2.80 mm^3 (IQR, 1.24; 9.76), $p = 0.49$.

d) Peritumoral edema volume

The median volume of edema was significantly different between the sham group and the treated groups, 0 mm³ vs. 25 mm³, $p < 0.01$. The volume of edema between the 2-fraction and 5-fraction groups showed an increasing trend, 19.6 mm³ (IQR, 8.8; 24.65) vs. 30.6 mm³ (IQR, 28.55; 45.3), $p = 0.066$.

Table 1 presents a summary of Δd , Δp , necrosis, edema and a cell death marker, which is represented here by a quantitative apoptosis marker measured using histology. As described by Leroy et al.¹⁰, this apoptosis marker was measured on slides digitized after immunohistochemistry using the TUNEL method (ApopTag[®] Plus Peroxidase In Situ, Millipore, USA). The statistical analyses revealed that this apoptosis marker was significantly increased in the 5-fraction group compared to the sham ($p = 0.024$) and 2-fraction groups ($p = 0.01$).

Table 1: Summary of Δd , Δp , necrosis, edema and a cell death marker represented by apoptosis marker data (TUNEL method)

	SHAM	2-FRACTION	5-FRACTION	<i>p</i> value
Δd	2.6% (IQR, 0.53, 5.39)	7.15% (IQR, -1.37, 18.1)	19% (IQR 9.6, 33.4)	<0.01
Δp	-23% (IQR -30.27; -15.31)	-36% (IQR, -70.15; -3.23)	-61% (IQR, -69.1; -49.5)	0.024
Apoptosis₁₀	1.28 (IQR 1.02; 1.58)	4.03 (IQR 3.53; 10.42)	30.35 (IQR 18.23; 47.51)	0.01 (2 vs. 5-fract)
Necrosis (mm³)	0	2.53 mm ³ (IQR, 0.67; 5.57)	2.80 mm ³ (IQR, 1.24; 9.76)	0.49 (2 vs. 5-fract)
Edema (mm³)	0	19.6 mm ³ (IQR, 8.8; 24.65)	30.6 mm ³ (IQR, 28.55; 45.3)	0.066 (2 vs. 5-fract)

Figures 3, 4 and 5 show examples of the 5-fraction and 2-fraction groups compared with no illumination on the tumor and adjacent parenchyma.

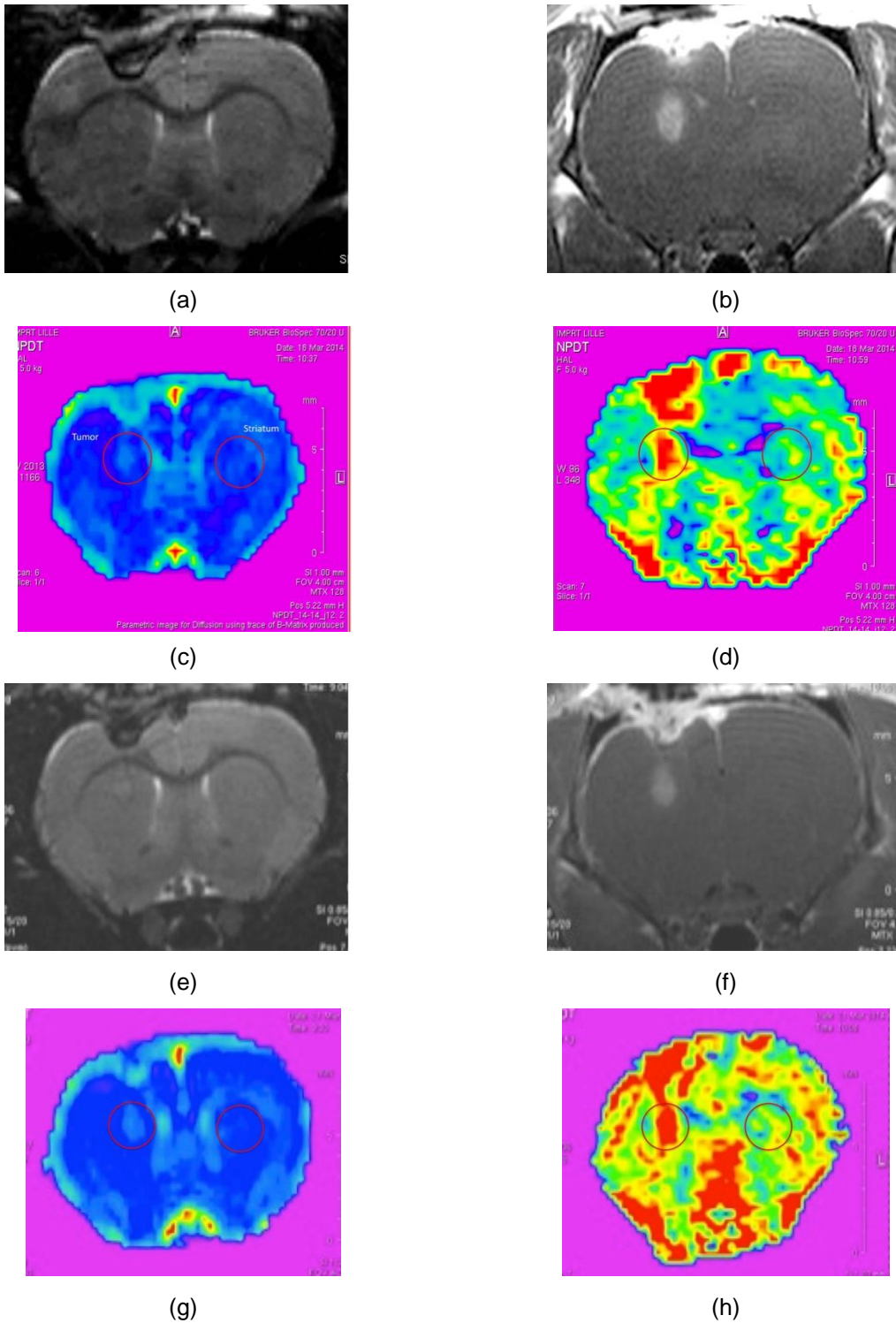


Figure 3: Pre- and postoperative MRI examination of rat #14, which belonged to the sham group. a) Preoperative T2 MRI, b) Preoperative with T1 with gadolinium MRI (T1 Gd), c) Preoperative diffusion MRI and d) Preoperative perfusion MRI. Postoperative MRI was performed 72 hours after the introduction of the fiber. (e): T2, lesion slightly hypointense without edema. (f): T1 Gd, clear contrast enhancement of the lesion. (g): Slight increase in diffusion within the tumor. (h): Hyperperfusion of the tumor tissue and cortex near the passage of the fiber.

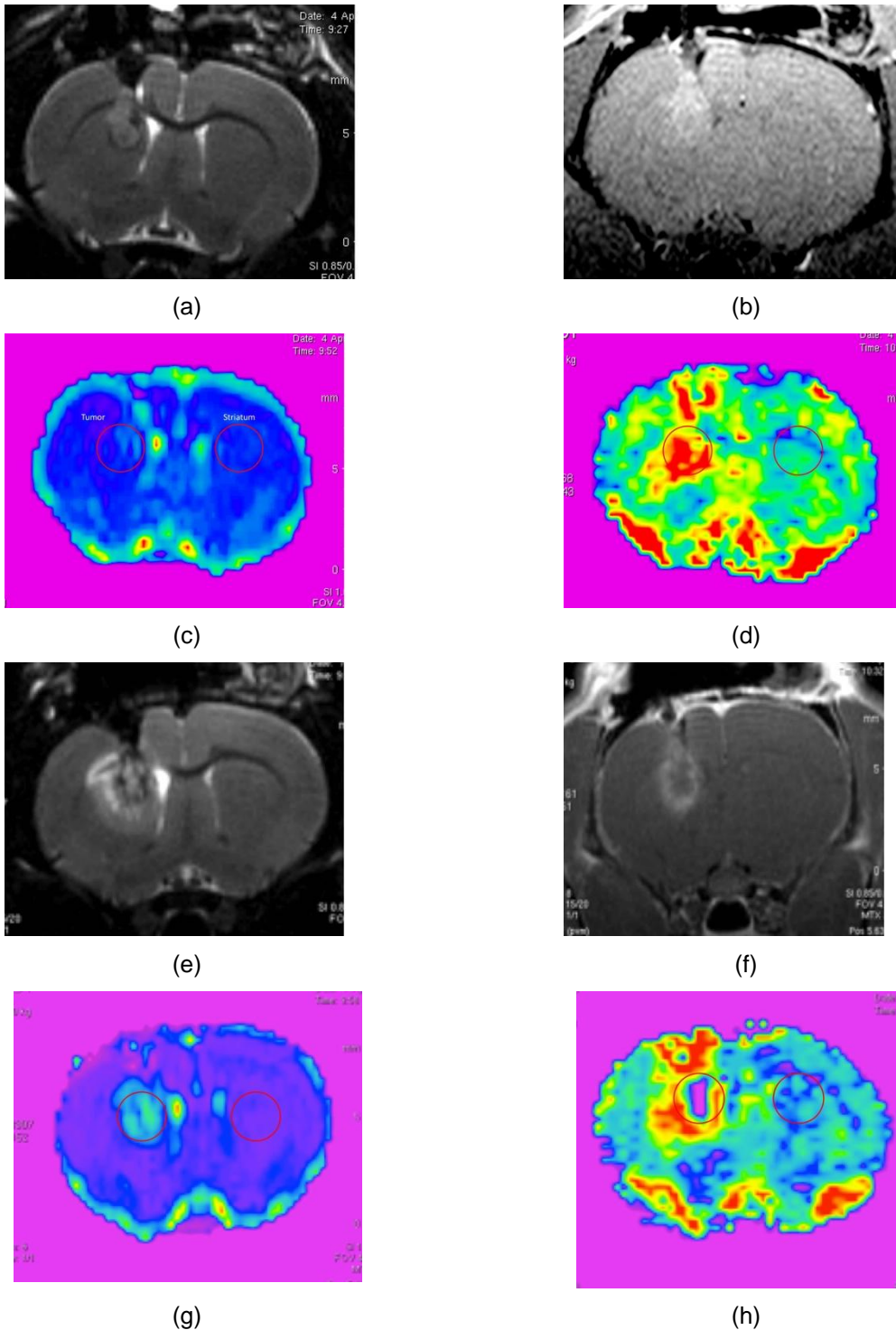


Figure 4: Pre- and postoperative MRI examination of rat #16, which belonged to the 2-fraction group. a) Preoperative T2 MRI, b) Preoperative with T1 Gd MRI (T1 Gd), c) Preoperative diffusion MRI and d) Preoperative perfusion MRI. Postoperative MRI was performed 72 hours after the 2-fraction treatment. (e): T2, heterogeneous lesion against the right putamen. (f): T1 Gd, contrast enhancement on the edge of the lesion, but not in the central part of the lesion. (g): Increase in the diffusion coefficient within the lesion, corresponding to necrosis induced by PDT. (h): Increase in perfusion in the peritumoral edema, contrasting with a sharp decrease in the central part of the tumor, confirming avascular necrosis induced by PDT.

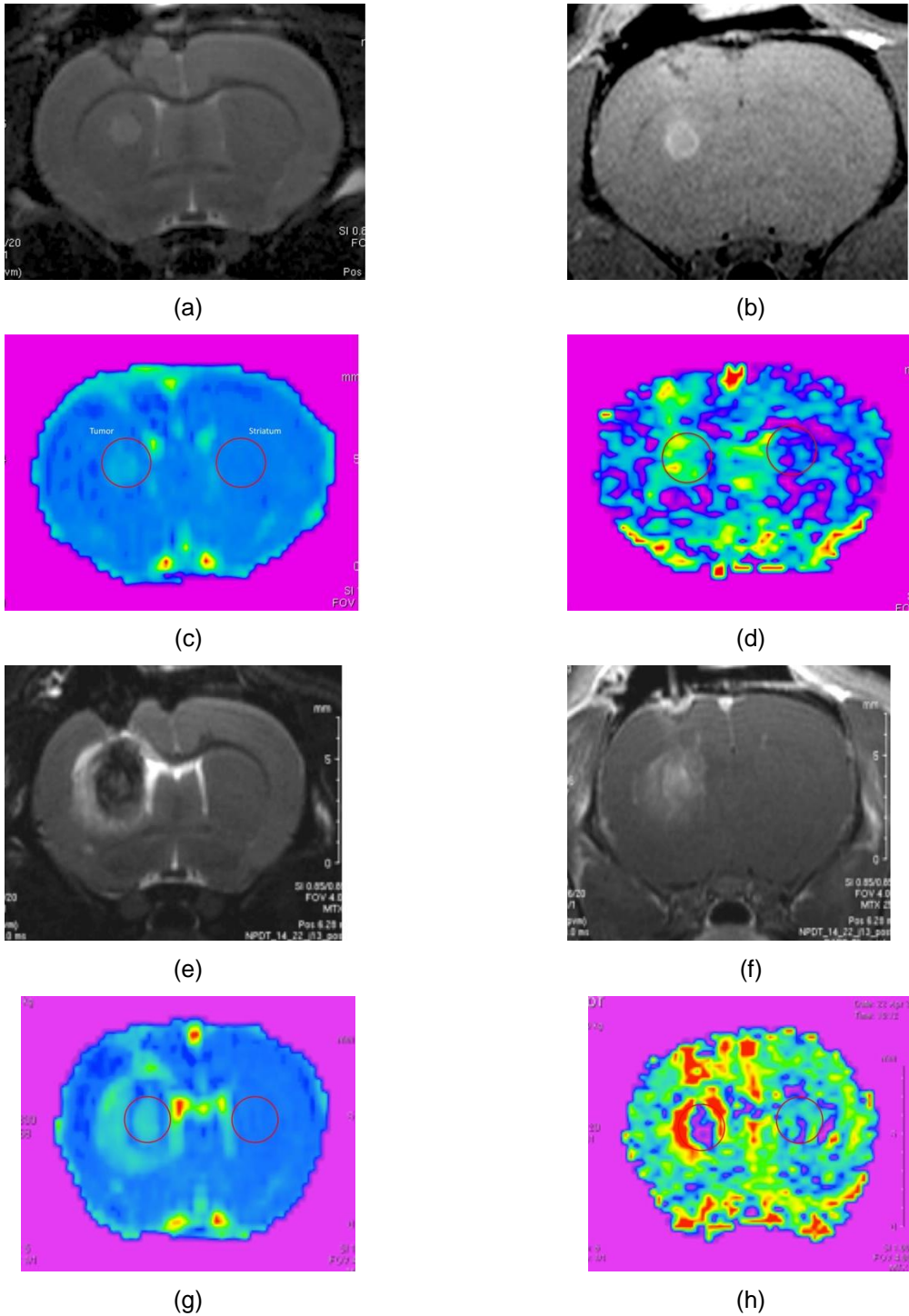


Figure 5: Pre- and postoperative MRI examination of rat #22, which belonged to the 5-fraction group. a) Preoperative T2 MRI, b) Preoperative with T1 Gd MRI (T1 Gd), c) Preoperative diffusion MRI and d) Preoperative perfusion MRI. Postoperative MRI was performed 72 hours after the 5-fraction treatment. (e): Large hyposignal area with peritumoral edema. (f): T1 Gd, poorly limited contrast enhancement, resulting in blood brain barrier alteration by the treatment. (g): Increase in the diffusion coefficient within the lesion, corresponding to the necrosis induced by PDT. (h): Increased perfusion in the peritumoral edema, contrasting with a sharp decrease in perfusion of the central part of the tumor,

confirming avascular necrosis induced by PDT.

Discussion

The objective of this study was to assess the radiological findings by comparing the MRI data, especially the diffusion and perfusion sequences, with the histological results. MRI data were collected from the same population for which histological results had been previously reported.

A significant difference in the distribution of Δd was found among the 3 groups, with an orderly increase from the sham to the 2-fraction and 5-fraction groups, ($p < 0.01$). In the sham group, the values remained stable with a slight increase (2.6%) after treatment, whereas these values increased up to 19% in the 5-fraction group. Increased diffusion values corresponded to accelerated movement of water molecules in the voxels of the studied matrix. We propose that this variation in Δd is caused by the cell death induced by PDT, including apoptosis or necrosis. Increased diffusion after PDT was also recently observed by Toussaint et al.¹⁷. This group reported an increase in the progression-free survival among rats with high apparent diffusion coefficients. Toussaint et al. shared our imaging platform for their MRI. These results obtained by two separate groups using different therapeutic protocols demonstrate the validity of diffusion imaging to assess the effectiveness of PDT. A previous immunohistological study of apoptosis¹⁰, reported in Table 1, also demonstrated a significant difference among the sham, 2-fraction and 5-fraction groups ($p = 0.01$). Additionally, the highest degree of apoptosis was found in specimens from the 5-fraction group ($p = 0.024$). This finding supports the hypothesis that the diffusion sequence can reflect cell death induced by PDT.

In a study by Leroy et al.¹⁰, the histological analysis revealed more extensive necrosis in the treated group than in the sham group ($p < 0.001$), and the extent of necrosis appeared greater in the 5-fraction group than the 2-fraction group, but without a significant difference. This result corroborates the MRI data detailed here.

Regarding Δp , a significant difference was observed with an orderly decrease from the sham to the 2-fraction and 5-fraction groups ($p = 0.024$). The decreased perfusion values reached -36% in the 2-fraction group and -61% in the 5-fraction group. Furthermore, vascular structures were no longer observed within the necrotic areas in the histological analysis, corroborating the decrease in perfusion values within the treated tumors. These results support a lesional effect of PDT on the tumor vasculature, as previously reported in the literature⁶. Yoshida et al. described post-PDT microvessel thrombosis that promoted focal ischemia, although they used Photofrin-mediated PDT, which is known to induce more vascular lesions than PpIX-mediated PDT²⁰. Toussaint et al. also reported a post-PDT hypoperfusion associated with improved progression-free survival¹⁷. Since the ROIs used the same positioning to calculate the variation in diffusion or perfusion, it was logical to also measure necrosis associated with hypoperfusion in that location. These results are similar to results obtained in human clinical studies^{7,18}.

On morphological MRI, the volume of necrosis was significantly different between the sham group and the treated groups ($p < 0.01$). However, no significant differences in the volume of necrosis were observed between the 2-fraction and 5-fraction groups ($p = 0.49$). Again, the same trend was reported for the histological data previously collected for the same population; the absence / presence of necrosis was significantly more predominant for the treated group ($p < 0.001$). Furthermore, our group previously showed the superiority of fractionated illumination vs. continuous illumination¹⁵ regarding necrosis.

Similar to the histological data in which peritumoral edema was observed significantly more often in the treated groups ($p = 0.009$), the administration of interstitial PDT was responsible for the increased peritumoral edema estimated on the T2 images compared to the sham group ($p < 0.01$). The volume of peripheral edema averaged 25 mm^3 , which represented a large volume compared to the average treated tumor volume of 4.7 mm^3 . Peripheral edema has been described as the main pitfall of PDT^{5,20}. Delivering five fractions of light tended to produce a volume of edema larger than that resulting from only two fractions of light.

Based on the immunohistology data, the MRI results appeared consistent, particularly for the extent of necrosis, rarefaction of the vascular pattern in the treated area, and perilesional edema. Furthermore, variation of the diffusion coefficient, as measured pre- and postoperatively, seems to be a reliable marker of apoptosis. Consequently, diffusion and perfusion MRI might be good predictive markers of treatment efficiency for apoptosis and necrosis. However, this preliminary study was conducted in a small number of animals, and the observations reported might form a basis for future exploratory studies to confirm the trends we observed. Additionally, no vascular staining results were provided, and staining of new vessels for vascular density (e.g., CD31) would be more suitable to correlate with the MRI results. Therefore, these MRI methods should be further explored in additional preclinical studies of survival to assess whether they might be useful as prognosis factors after administration of PDT.

Conclusion

A previous study reported that fractionated interstitial 5-ALA PDT induces targeted tumor lesions¹⁵. The primary effects included necrosis, apoptosis, and reduced central tumor vascularization, as confirmed by immunohistology. In the current study, we observed that diffusion and perfusion sequences accurately assess the treatment effects. Indeed, diffusion was a relevant marker of cell death, and perfusion robustly described the level of necrosis. The 5-fraction protocol was associated with a higher Δd and a lower Δp . This finding corroborates our previous histological findings depicting an improved lesional effect of the 5-fraction scheme compared with the 2-fraction protocol¹⁰. As expected, T2 MRI was clearly confirmed to be a precise peritumoral edema estimator. These sequences could be used to non-invasively predict the histological lesions induced by interstitial PDT and facilitate patient monitoring.

Finally, despite the use of the same cohort for histological and MRI analyses, the results were based only on a comparison of group averages rather than a spatially resolved analysis. At this early stage, a spatially resolved analysis remains difficult to achieve because of image registration issues, such as different spatial resolution and 3D images from MRI vs. 2D images from histology, which might have interfered with the final results. However, such a spatially resolved analysis is critically necessary to support our results and is the aim of a future study.

References

1. Beck TJ, Kreth FW, Beyer W, Mehrkens JH, Obermeier A, Stepp H, Stummer W, Baumgartner R: Interstitial photodynamic therapy of nonresectable malignant glioma recurrences using 5-aminolevulinic acid induced protoporphyrin IX. **Lasers in surgery and medicine** **39**:386-393, 2007
2. Candolfi M, Curtin JF, Nichols WS, Muhammad AG, King GD, Pluhar GE, McNiel EA, Ohlfest JR, Freese AB, Moore PF, Lerner J, Lowenstein PR, Castro MG: Intracranial glioblastoma models in preclinical neuro-oncology: neuropathological characterization and tumor progression. **Journal of neuro-oncology** **85**:133-148, 2007
3. Curnow A, Haller JC, Bown SG: Oxygen monitoring during 5-aminolaevulinic acid induced photodynamic therapy in normal rat colon: comparison of continuous and fractionated light regimes. **Journal of Photochemistry and Photobiology**:58 149-155, 2000
4. Curnow A, McIlroy BW, Postle-Hacon MJ, MacRobert AJ, Bown SG: Light dose fractionation to enhance photodynamic therapy using 5-aminolevulinic acid in the normal rat colon. **Photochemistry and photobiology** **69**:71-76, 1999
5. Dereski MO, Chopp M, Chen Q, Hetzel FW: Normal brain tissue response to photodynamic therapy: histology, vascular permeability and specific gravity. **Photochemistry and photobiology** **50**:653-657, 1989
6. Henderson BW, Dougherty TJ: How does photodynamic therapy work? **Photochem Photobiol** **55**:145-157, 1992
7. Hu LS, Eschbacher JM, Heiserman JE, Dueck AC, Shapiro WR, Liu S, Karis JP, Smith KA, Coons SW, Nakaji P, Spetzler RF, Feuerstein BG, Debbins J, Baxter LC: Reevaluating the imaging definition of tumor progression: perfusion MRI quantifies recurrent glioblastoma tumor fraction, pseudoprogression, and radiation necrosis to predict survival. **Neuro-oncology** **14**:919-930, 2012
8. Iacob G, Dinca EB: Current data and strategy in glioblastoma multiforme. **Journal of medicine and life** **2**:386-393, 2009
9. Jemal A, Siegel R, Ward E, Hao Y, Xu J, Murray T, Thun MJ: Cancer statistics, 2008. **CA Cancer J Clin** **58**:71-96, 2008
10. Leroy HA, Vermandel M, Vignion-Dewalle AS, Leroux B, Maurage CA, Duhamel A, Mordon S, Reyns N: Interstitial photodynamic therapy and glioblastoma: Light fractionation in a preclinical model. **Lasers Surg Med** **49**:506-515, 2017
11. Omuro A, DeAngelis LM: Glioblastoma and other malignant gliomas: a clinical review. **JAMA** **310**:1842-1850, 2013
12. Ostrom QT, Bauchet L, Davis FG, Deltour I, Fisher JL, Langer CE, Pekmezci M, Schwartzbaum JA, Turner MC, Walsh KM, Wrensch MR, Barnholtz-Sloan JS: The epidemiology of glioma in adults: a "state of the science" review. **Neuro-oncology** **16**:896-913, 2014
13. Schuierer G, Reimer P, Allkemper T, Peters PE: [Fast and ultra-fast MRI of the brain]. **Radiologe** **35**:894-901, 1995
14. Stummer W, Beck T, Beyer W, Mehrkens JH, Obermeier A, Etminan N, Stepp H, Tonn Jr-CC, Baumgartner R, Herms J, Kreth FW: Long-sustaining response in a patient with non-resectable, distant recurrence of glioblastoma multiforme treated by interstitial photodynamic therapy using 5-ALA: case report. **Journal of neuro-oncology** **87**:103-109, 2008

15. Tetard MC, Reyns N, Leroy HA, Lejeune JP, Mordon S, Vermandel M: Light Dose Fractionation to Enhance Photodynamic Therapy With 5-Aminolevulinic Acid in Human glioma xenografts., in **The International Congress on Photodynamic Applications (ICPA 2014)** Dundee, Scotland, 2014
16. Tetard MC, Vermandel M, Leroy HA, Leroux B, Maurage CA, Lejeune JP, Mordon S, Reyns N: Interstitial 5-ALA photodynamic therapy and glioblastoma: Preclinical model development and preliminary results. **Photodiagnosis Photodyn Ther** **13**:218-224, 2016
17. Toussaint M TM, Amouroux M, Bastogne T, Frochet C, Mordon S, Barberi-Heyob M: Optimization of illumination in interstitial photodynamic therapy for high-grade brain tumors, in **International Congress on Photodynamic Applications**. Dundee, UK, 2014
18. Tran DK, Jensen RL: Treatment-related brain tumor imaging changes: So-called "pseudoprogression" vs. tumor progression: Review and future research opportunities. **Surgical neurology international** **4**:35, 2013
19. Wong EC, Buxton RB, Frank LR: Implementation of quantitative perfusion imaging techniques for functional brain mapping using pulsed arterial spin labeling. **NMR in biomedicine** **10**:237-249, 1997
20. Yoshida Y, Dereski MO, Garcia JH, Hetzel FW, Chopp M: Neuronal injury after photoactivation of photofrin II. **The American journal of pathology** **141**:989-997, 1992